Analysis and Design of Integrated Control for Multi-Axis Motion Systems

Syh-Shiuh Yeh and Pau-Lo Hsu

***Abstract*—In modern manufacturing, the design of multi-axis motion controllers for high-speed/high-precision and complex machining is becoming more critical. In the past, controllers for each axis were, in general, designed individually to obtain desirable tracking accuracy. Although some advanced motion control algorithms have been developed recently, they are mostly applicable to single-axis or biaxial systems. In particular, the design of two-axis integrated control, which includes: 1) feedback loops; 2) feedforward loops; and 3) the cross-coupled control (CCC), achieves significantly improved performance. However, its applications are limited to basic linear and circular contour commands for two-axis systems only. In this paper, system analysis for the multi-axis integrated control structure is proposed in order to achieve tracking and contouring accuracy simultaneously. With the derived contouring error transfer function (CETF), the integrated control design for multi-axis motion systems can be formulated simply as a single-input–single-output (SISO) design. Thus, a robust design with desirable performance for multi-axis motion systems can then be achieved straightforwardly. Moreover, by estimating the contouring error vector, the proposed multi-axis integrated control can be widely applied to general contour commands. Experimental results on a three-axis CNC machining center indicate that both tracking and contouring accuracy are simultaneously improved by applying the proposed control design.**

***Index Terms*—Contouring accuracy, cross-coupled control (CCC), feedforward control, integrated control, tracking accuracy.**

I. Introduction

In general multi-input–multi-output (MIMO) systems, multivariable control theories are applied to minimize the tracking error while maintaining satisfactory stability margins for each control variable. However, in multi-axis manufacturing systems, motion precision is determined by both the tracking accuracy and the contouring accuracy, as shown in Fig. 1. In multi-axis systems, although feedback and feedforward control loops for each axis can be individually designed for each axis to achieve enhanced tracking accuracy, a controller which minimizes the mutual dynamic effects among the multiple axes is desired in order to improve both tracking and contouring accuracy. Poo *et al.* [1] indicated that matching open-loop gains among axes results in better contouring performance. On the other hand, feedforward control designs have been shown to reduce servo lag and tracking errors. In particular, Tomizuka proposed the zero phase-error tracking control (ZPETC) [2] and several modified ZPETCs have subsequently been proposed to improve tracking performance [3]–[5].

Manuscript received June 20, 2001. Manuscript received in final form January 6, 2003. Recommended by Associate Editor S. K. Agrawal. This work was supported by National Science Council under Grant NSC 88-2212-E-009-026.

S.-S. Yeh was with the Department of Electrical and Control Engineering, National Chiao Tung University, Hsinchu, Taiwan, R.O.C. He is now with the Mechanical Industry Research Laboratory, Industrial Technology Research Institute, Hsinchu, Taiwan, R.O.C.

P.-L. Hsu is with the Department of Electrical and Control Engineering, National Chiao Tung University, Hsinchu, Taiwan, R.O.C.

Digital Object Identifier 10.1109/TCST.2003.810372

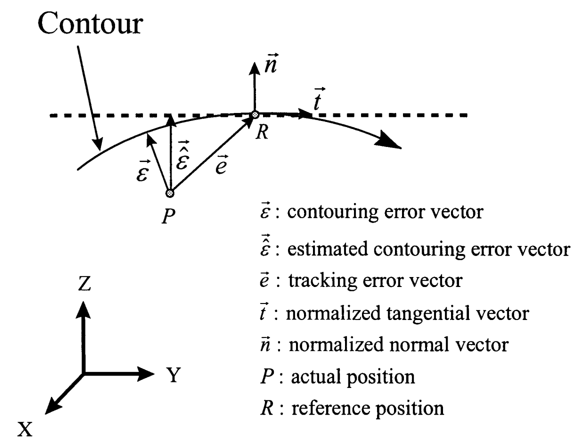

Fig. 1. Tracking error and the contouring error for multi-axis systems.

Feedback and feedforward control loops have been applied to each axis to improve tracking accuracy. In contrast, the cross-coupled control (CCC) structure, which considers the mutual dynamic effects among all axes, was developed mainly to reduce the contouring error [6]. Various CCCs were then proposed for biaxial systems [7]–[12]. However, it is difficult to extend the available CCCs, derived simply from geometrical approximations of the contouring error, to multi-axis motion systems with arbitrary contour commands.

Recently, Lo [13] proposed an feedback control approach for three-axis motion systems. This approach involves transforming the coordinates to obtain the moving basis. Chiu and Tomizuka [14] proposed a task coordinated approach by considering all axes as the first-order loops to obtain feedback and feedforward control loops. However, Lo's approach is difficult to apply and since it lacks a feedforward control loop, its tracking accuracy can be further improved. On the other hand, performance of a first-order model design like Chiu and Tomizuka's is inherently limited in real applications. In fact, the integrated control which includes different control structures has been proven to provide the most reliable performance for bi-axial systems [15], [16].

In this paper, we use the estimated contouring error vector to obtain the variable cross-coupling gains of CCC for multi-axis systems [17]. Furthermore, we analyze the control structure with integration of: 1) feedback control; 2) feedforward control; and 3) the multi-axis CCC. Analytical results indicate that a simple controller design algorithm can be obtained by applying a novel formulation of the contouring error transfer function (CETF) for multi-axis motion systems. Thus, robust integrated controllers can be achieved with highly improved both tracking and contouring accuracy. Experimental results on a three-axis industrial DYNA 1007 CNC machine tool are provided to

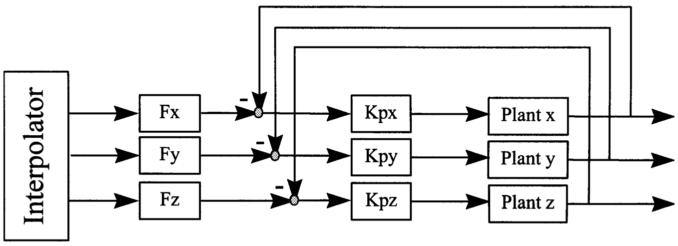

Fig. 2. Feedback and feedforward control for multi-axis motion systems.

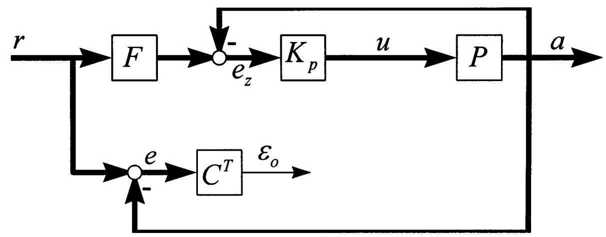

Fig. 3. Equivalent 2-DOF control structure of a multi-axis motion system.

verify that the proposed control design significantly improves motion accuracy.

II. Analysis of Multi-Axis Systems

A. Design With Individual Axis

In manufacturing processes such as machining, quality is determined by both tracking and contouring motion accuracy. Traditionally, accuracy of motion systems is improved by applying feedback controller (Kpx, Kpy, Kpz) or feedforward controller (Fx, Fy, Fz) for each axis as shown in Fig. 2. For feedback controllers, one may use PID, lead-lag, or modern control designs to reduce tracking error of each axis. The matched dc gain was proposed by Poo *et al.* [1] to improve contouring accuracy in operations at low speeds. Recently, the perfectly matched feedback control design for multi-axis motion systems was developed through the whole frequency range [18]. To further reduce tracking error caused by the servo lag for each axis, the ZPETC or optimal ZPETC is suitable feedforward control design.

To analyze tracking and contouring errors, consider the general multi-axis motion control system as shown in Fig. 3. Here, e and ε denotes the tracking error and the contouring error, respectively. To analyze the errors with and without CCC, the contouring error is further denoted as ε_c and ε_o, respectively. Other terms are as follows:

$r=[r_1 r_2 \cdots r_n]^T$, $r_i, i=1,\ldots,n$	Axial reference position command.
$e=[e_1 e_2 \cdots e_n]^T$, $e_i, i=1,\ldots,n$	Axial position error.
$e_z=[e_{z1} e_{z2} \cdots e_{zn}]^T$, $e_{zi}, i=1,\ldots,n$	Filtered axial position error.
$u=[u_1 u_2 \cdots u_n]^T$, $u_i, i=1,\ldots,n$	Axial driving signal.
$a=[a_1 a_2 \cdots a_n]^T$, $a_i, i=1,\ldots,n$	Actual axial position.
$F=\mathrm{diag}\{F_1, F_2, \ldots, F_n\}$, $F_i, i=1,\ldots,n$	Feedforward controller of each axis.
$K_p = \mathrm{diag}\{K_{p1}, K_{p2}, \ldots, K_{pn}\}$, $K_{pi}, i=1,\ldots,n$	Position feedback controller of each axis.
$P=\mathrm{diag}\{P_1, P_2, \ldots, P_n\}$, $P_i, i=1,\ldots,n$	Controlled plant of each axis.
$C=[C_1 C_2 \cdots C_n]^T$	Column vector of geometrical relationships between the tracking and contouring errors.

Since

$$
\begin{aligned}
e_z &= F \cdot r - a; \quad u = K_p \cdot e_z \\
a &= P \cdot u; \quad e = r - a
\end{aligned}
$$

the tracking error e and the contouring error ε_o are derived as

$$
e = (I + PK_p)^{-1} \cdot (I + PK_p - PK_pF) \cdot r \tag{1}
$$

$$
\begin{aligned}
\varepsilon_o &= C^T \cdot e = C^T \cdot (I + PK_p)^{-1} \\
&\quad \cdot (I + PK_p - PK_pF) \cdot r.
\end{aligned} \tag{2}
$$

Equations (1) and (2) show that the tracking and contouring errors can be reduced through a suitable choice of the position loop controller K_p and the feedforward controller F.

B. Design With Cross-Coupled Control

In addition to feedback and feedforward control loops for each axis, we will consider the cross-coupled control (CCC) structure [6], [10], [11] which takes into account the dynamic effects among all the axes. Recently, Yeh and Hsu [15] integrated the bi-axial CCC, feedback and feedforward controllers to significantly improve both tracking and contouring accuracy in motion systems with only two axes. To extend this approach to pursue accuracy of systems with multiple axes, we introduce the multi-axis integrated structure which combines: 1) feedback controllers (Kpx, Kpy, Kpz); 2) feedforward controllers (Fx, Fy, Fz); and 3) the cross-coupled controller, as shown in Fig. 4. The solid lines represent the feedback and feedforward loops, and the dashed lines denote the multi-axis CCC structure. (Cx, Cy, Cz) are cross-coupling gains and $\|\vec{\hat{\varepsilon}}\|$ denotes the estimated contouring error.

Fig. 5 shows the equivalent structure of the multi-axis integrated control system in Fig. 4. ε_c denotes the estimated contouring error of the system *with* the CCC structure and K_c is the cross-coupled controller. Note that ε_o, as in (2), is the estimated contouring error *without* the CCC.

C. Formulation of the Multi-Axis Integrated Control

The terms in Fig. 5 are

$$
\begin{aligned}
u &= K_p \cdot e_z + C \cdot K_c \cdot C^T \cdot e; \quad a = P \cdot u \\
e_z &= F \cdot r - a; \quad e = r - a.
\end{aligned}
$$

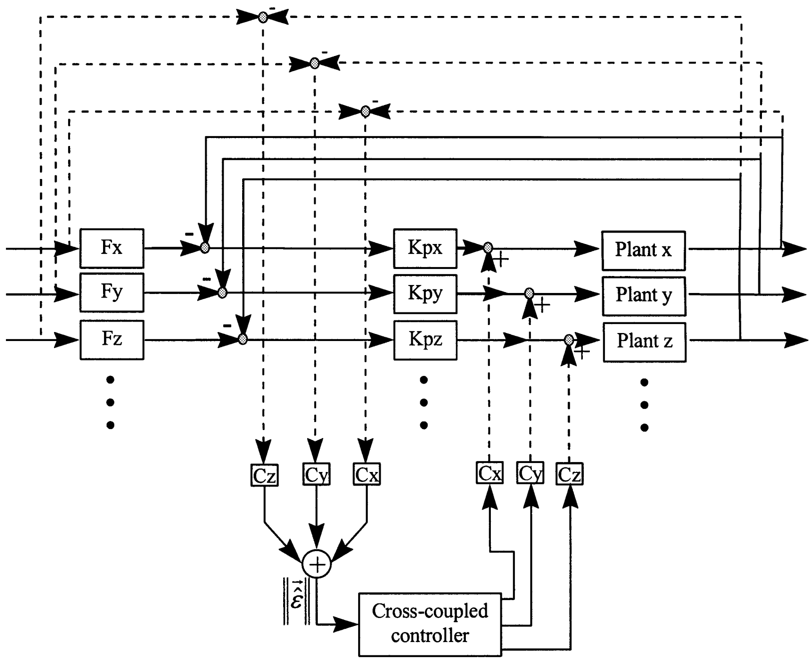

Fig. 4. Multi-axis integrated control system.

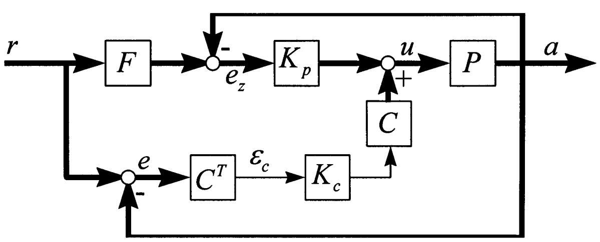

Fig. 5. Equivalent structure of the multi-axis integrated control system.

By applying the multi-axis CCC, the output signal a, the error signal e, and the contouring error signal ε_c are derived as

$$a = \left(I + PK_p + PCK_cC^T\right)^{-1} \cdot \left(PK_pF + PCK_cC^T\right) \cdot r \quad (3)$$

$$e = \left(I + PK_p + PCK_cC^T\right)^{-1} \cdot \left(I + PK_p - PK_pF\right) \cdot r \quad (4)$$

$$\varepsilon_c = C^T \cdot e = C^T \cdot \left(I + PK_p + PCK_cC^T\right)^{-1} \cdot \left(I + PK_p - PK_pF\right) \cdot r. \quad (5)$$

Equations (4) and (5) indicate that the feedforward controller F, the feedback controller K_p and the cross-coupled controller K_c can be designed to simultaneously minimize the tracking error e and the contouring error ε_c. The feedforward controller F and feedback controller K_p can be designed simply by using proportional integral derivative (PID) and ZPETC, respectively. However, design for the multi-axis CCC, including the variable gains C_i and the controller K_c, have not been previously developed.

III. Variable Gains of the Multi-Axis CCC

Koren and Lo proposed the variable-gain CCC for bi-axial system with simple geometrical relationships between the tracking error and the contouring error [10], [11]. However, the method was developed for biaxial systems cannot be directly applied to motion systems with multiple axes. In the present approach, a new algorithm featuring real-time estimation of the contouring error vector is adopted to determine the CCC variable gains [17].

Consider the geometric relations among an arbitrary contour, the actual position P, and the reference position R in three-dimensional (3-D) space as shown in Fig. 1. In multi-axis CCC, we wish to minimize the contouring error by applying suitable compensation components to each axis. In general, it is difficult to obtain the exact contouring error vector $\vec{\varepsilon}$ in real time for multi-axis systems. However, the magnitude and direction of the contouring error vector $\vec{\varepsilon}$, as shown in Fig. 1, can be approximated simply by the estimated contouring error vector $\vec{\hat{\varepsilon}}$. $\vec{\hat{\varepsilon}}$ is defined as a vector from the actual position P to the nearest point on the line passing through reference position R with tangential direction $\vec{t}$. The estimated contouring error vector $\vec{\hat{\varepsilon}}$ lies on the plane expanded by the tracking error vector $\vec{e}$ and the normalized tangential vector $\vec{t}$, and is perpendicular to the normalized tangential vector $\vec{t}$. In fact, when the tracking error $\|\vec{e}\|$ of the motion systems is small enough, the contouring error vector $\vec{\varepsilon}$ can be properly approximated by the estimated contouring error vector $\vec{\hat{\varepsilon}}$. Define the normalized estimated contouring error vector $\vec{n}$ as

$$\vec{n} = \alpha_1\vec{t} + \alpha_2\vec{e} \quad (6)$$

where

$$\langle \vec{n}, \vec{t} \rangle = 0 \quad (7)$$

$$\|\vec{n}\| = 1 \text{ or } \langle \vec{n}, \vec{n} \rangle = 1 \tag{8}$$
$$\left\|\vec{t}\right\| = 1. \tag{9}$$

The relation between α_1 and α_2 can be derived from (7)–(9) as

$$\alpha_1 = -\alpha_2 \cdot \langle \vec{e}, \vec{t} \rangle . \tag{10}$$

By substituting (10) into (8) with the practical limit that the angle between this vector and the tracking error vector is within $[-90^\circ, +90^\circ]$, α_1 and α_2 are obtained as

$$\alpha_1 = -\frac{\langle \vec{e}, \vec{t} \rangle}{\sqrt{\|\vec{e}\|^2 - \langle \vec{e}, \vec{t} \rangle^2}} \tag{11}$$
$$\alpha_2 = \frac{1}{\sqrt{\|\vec{e}\|^2 - \langle \vec{e}, \vec{t} \rangle^2}}. \tag{12}$$

As shown in (6), the magnitude of the estimated contouring error vector is the inner product between the normalized estimated contouring error vector and the tracking error vector

$$\left\|\vec{\hat{\varepsilon}}\right\| = \langle \vec{n}, \vec{e} \rangle . \tag{13}$$

Where $\vec{n} = [n_x \quad n_y \quad n_z \quad \cdots]^T$. The compensation direction for a given axis is the cross-coupling gain in the CCC. As long as the tracking error is small enough, the cross-coupling gains can be directly obtained as the elements of the normalized estimated contouring error vector. The cross-coupling gains $(C_x \quad C_y \quad C_z \quad \cdots)$ for multi-axis motion systems are, thus, directly determined as

$$C_i = n_i, \quad i = x, y, z, \ldots .$$

IV. Design of the CCC in the Integrated Control

A. Multi-Axis Contouring Error Transfer Function

Applying the inversion lemma to (5), we have

$$\begin{aligned}&\left(I + PK_p + PCK_cC^T\right)^{-1}\\ &\quad = (I + PK_p)^{-1} - (I + PK_p)^{-1}\\ &\quad\quad \cdot \left[P^{-1} + CK_cC^T (I + PK_p)^{-1}\right]^{-1}\\ &\quad\quad \cdot CK_cC^T (I + PK_p)^{-1} .\end{aligned} \tag{14}$$

By substituting (14) and (2) into (5), a relation between the estimated contouring error, *with* and *without* the CCC denoted as ε_c and ε_o, is obtained as

$$\varepsilon_c = \left\{1 - C^T (I + PK_p)^{-1} \cdot \left[P^{-1} + CK_cC^T (I + PK_p)^{-1}\right]^{-1} CK_c\right\} \varepsilon_o. \tag{15}$$

Since

$$\begin{aligned}&1 - C^T (I + PK_p)^{-1} \cdot \left[P^{-1} + CK_cC^T (I + PK_p)^{-1}\right]^{-1} CK_c\\
&= 1 - C^T (I + PK_p)^{-1} \cdot \left[K_c^{-1}P^{-1} + CC^T (I + PK_p)^{-1}\right]^{-1} C\\
&= 1 - C^T (I + PK_p)^{-1} \cdot \left\{\left[K_c^{-1}P^{-1} (I + PK_p) + CC^T\right] (I + PK_p)^{-1}\right\}^{-1} C\\
&= 1 - C^T \left[K_c^{-1}P^{-1} (I + PK_p) + CC^T\right]^{-1} C\\
&= \left[1 + C^T (I + PK_p)^{-1} PK_cC\right]^{-1}\\
&= \frac{1}{1 + C^T (I + PK_p)^{-1} PK_cC}.\end{aligned}$$

Equation (15) can be represented in a more compact form as

$$\varepsilon_c = \frac{1}{1 + C^T (I + PK_p)^{-1} PK_cC} \varepsilon_o. \tag{16}$$

Define the equivalent controlled plant K, in which all models and parameters are known, and the desirable transfer function T as

$$\begin{aligned}K &= C^T (I + PK_p)^{-1} PC\\ T &= \frac{1}{1 + C^T (I + PK_p)^{-1} PK_cC} = \frac{1}{1 + KK_c}\end{aligned} \tag{17}$$

then, (16) can be further represented as

$$\varepsilon_c = T \cdot \varepsilon_o. \tag{18}$$

The transfer function T is named the contouring error transfer function (CETF). It constitutes the response of contouring error between *with* and *without* the multi-axis CCC [15]. From (18), it is clearly desirable to design a cross-coupled controller K_c so that the contouring error ε_o can be further reduced to ε_c. The control design problem for the multi-axis motion system now becomes the general single-input-single-output (SISO) control design for obtaining a desirable sensitivity function T.

By including the feedback loop, the feedforward loop, and the proposed multi-axis CCC, we obtain an integrated control which minimizes both tracking and contouring errors. The design is summarized as follows.

Algorithm: The Integrated Controller Design
Step 1. Design the feedback controller K_p individually for each axis with matched dynamic properties.
Step 2. Design the feedforward controller F for each axis to reduce the tracking error.
Step 3. Design the cross-coupled controller K_c and the CETF to further reduce the contouring error.

B. Stability Analysis

The stability of the multi-axis integrated control system is considered in the following lemma.

Lemma: If the multi-axis integrated controlled system is designed to meet the following requirements:

(A1) the position loops which include feedback and feedforward controllers as shown in Fig. 3 are designed to be bounded-input–bounded-output (BIBO) stable;
(A2) the CETF T remains stable as the cross-coupling gains are varied;

then the designed multi-axis integrated control system is BIBO stable.

Proof: Since the tracking error as in (4) is

$$\begin{aligned} e =& r - a \\ =& \left(I + PK_p + PCK_cC^T\right)^{-1} \cdot (I + PK_p - PK_pF) \cdot r \\ =& \left(I + PK_p + PCK_cC^T\right)^{-1} \cdot (I + PK_p) \\ & \cdot \left[I - (I + PK_p)^{-1} PK_pF\right] \cdot r \\ =& \left[I - \left(I + PK_p + PCK_cC^T\right)^{-1} PCK_cC^T\right] \\ & \cdot \left[I - (I + PK_p)^{-1} PK_pF\right] \cdot r \end{aligned} \tag{19}$$

and the CETF is

$$\begin{aligned} T =& \left[1 + C^T (I + PK_p)^{-1} PK_cC\right]^{-1} \\ =& 1 - C^T \left(I + PK_p + PCK_cC^T\right)^{-1} PCK_c \end{aligned} \tag{20}$$

the characteristic roots of the integrated system can be divided into two parts: 1) the term $\left|I - (I + PK_p)^{-1} PK_pF\right|$, which is determined by the position loops and 2) the term $\left|I - \left(I + PK_p + PCK_cC^T\right)^{-1} PCK_cC^T\right|$, which is determined by the CCC loop as shown in (19). Since all the designed feedback loops, feedforward loops, and CCC meet requirements (A1) and (A2), all poles of the integrated multi-axis system are stable and the system is, thus, BIBO stable.

Because the multi-axis CCC includes cross-coupling gains which vary within the range $[-1, 1]$ and depend on the path trajectory, the integrated system under discussion is a parameter-varying motion system. In general, the stability of parameter-varying systems is guaranteed when parameters vary slowly [19], [20]. In practice, multi-axis motion control systems are typically applied to processes with slow contour motion such as fine machining.

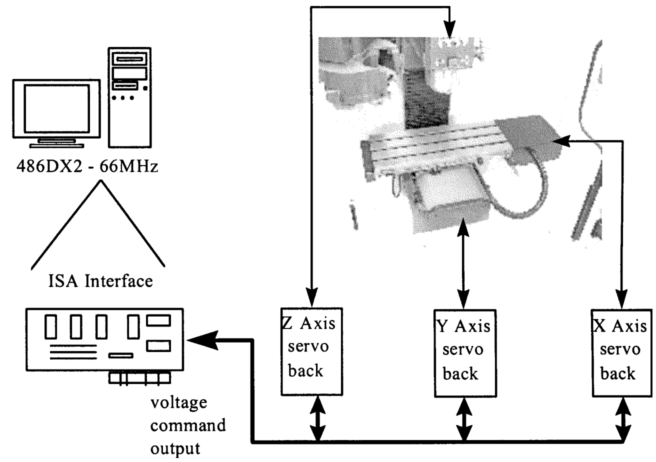

Fig. 6. Experimental setup.

V. Experiments

A. Experimental Setup

The experimental setup of a three-axis DYNA 1007 CNC machine center is shown in Fig. 6. A PC-486 generated the main control commands and recorded the signals including: the input commands for different contours, the implementation of a variable-gain CCC, and the control inputs to the velocity loop of the AC servo motors. The PC-486 interface utilized an AD/DA card to send and receive the control input and position output at a sampling period of 1 ms.

To identify the controlled plant of each axis, the axial control input was given a pseudorandom binary sequence (PRBS) and the plant was modeled using the ARX model [21] as shown in the equation at the bottom of the page.

B. Control Design

The following four control structures were tested:

Case 1) system with P feedback control only (feedback);
Case 2) system with feedback and feedforward control (feedforward);
Case 3) system with feedback control and multi-axis CCC (CCC);
Case 4) system with integrated controller including feedback, feedforward, and CCC (Integrated).

To achieve both stable motion and matched dynamic properties for the uncoupled system [1], the proportional position feedback controllers (K_{p1}, K_{p2}, K_{p3}) were set at

$$K_{p1} = 0.07; \quad K_{p2} = 0.0694; \quad K_{p3} = 0.0665.$$

$$\begin{aligned} P_1\left(z^{-1}\right) =& \frac{-0.0056z^{-1} + 0.0421z^{-2} + 0.1213z^{-3} + 0.0922z^{-4}}{1 - 1.1087z^{-1} - 0.2199z^{-2} + 0.1578z^{-3} + 0.0452z^{-4} + 0.1484z^{-5} - 0.0228z^{-6}} \\ P_2\left(z^{-1}\right) =& \frac{-0.0015z^{-1} + 0.0445z^{-2} + 0.1251z^{-3} + 0.0586z^{-4}}{1 - 1.2360z^{-1} - 0.1549z^{-2} + 0.2173z^{-3} + 0.0723z^{-4} + 0.2628z^{-5} - 0.1616z^{-6}} \\ P_3\left(z^{-1}\right) =& \frac{-0.0150z^{-1} + 0.0522z^{-2} + 0.1404z^{-3} - 0.0207z^{-4}}{1 - 1.6425z^{-1} + 0.3038z^{-2} + 0.4394z^{-3} - 0.1691z^{-4} + 0.1897z^{-5} - 0.1213z^{-6}}. \end{aligned}$$

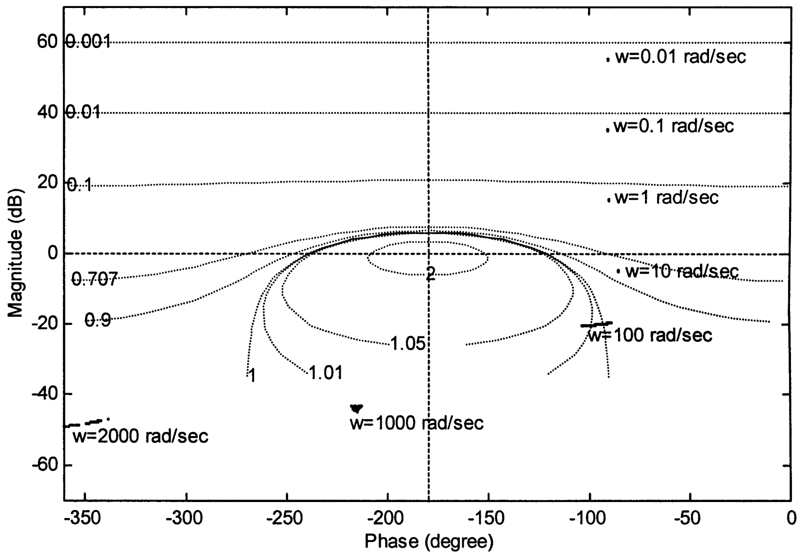

Fig. 7. Frequency responses of KK_c.

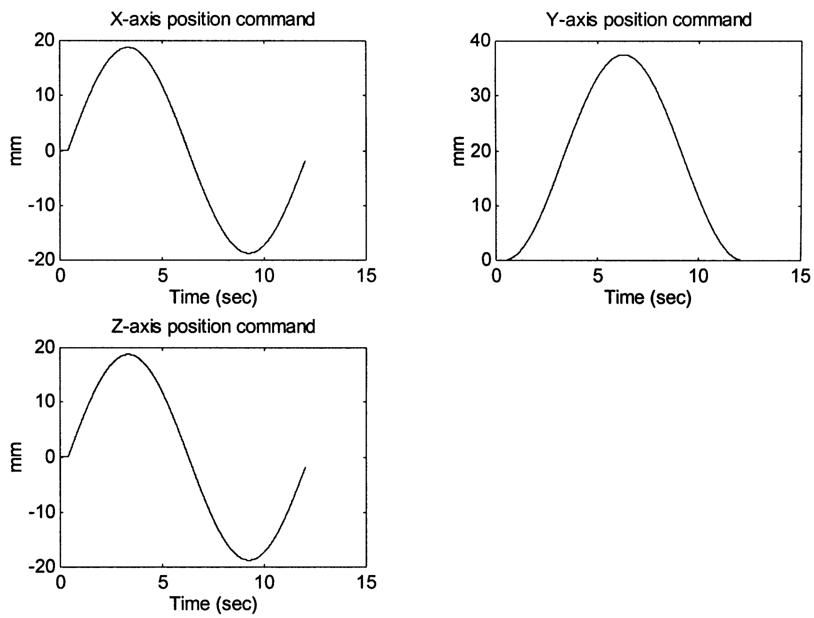

Fig. 8. Three-axis contour commands[17].

To further reduce tracking errors, the optimal ZPETC [5] was applied to each axis (F_1, F_2, F_3) as shown in the equation at the bottom of the page.

Then, we designed the multi-axis CCC. To maintain system stability as cross-coupling gains vary, the designed gain margin and phase margin were chosen as 40 dB and 90°, respectively.

$$F_1\left(z^{-1}\right) = \frac{\begin{array}{c} -1.4572z^7 + 11.4286z^6 - 37.7882z^5 + 62.5618z^4 + 18.1900z^3 - 68.7539z^2 - 12.5623z^1 \\ 23.6911z^0 + 2.1475z^{-1} + 4.9953z^{-2} - 0.8071z^{-3} - 1.4200z^{-4} + 1.0685z^{-5} - 0.3366z^{-6} \\ 0.0446z^{-7} - 0.0020z^{-8} \end{array}}{1}$$

$$F_2\left(z^{-1}\right) = \frac{\begin{array}{c} 0.1532z^7 - 2.0391z^6 + 12.8177z^5 - 51.5861z^4 + 164.5193z^3 - 117.2762z^2 - 63.6212z^1 \\ 41.5541z^0 - 2.3471z^{-1} + 37.1148z^{-2} - 13.5447z^{-3} - 6.2384z^{-4} + 2.8238z^{-5} - 0.8884z^{-6} \\ 0.1734z^{-7} - 0.0168z^{-8} + 0.0004z^{-9} \end{array}}{1 + 0.5988z^{-1}}$$

$$F_3\left(z^{-1}\right) = \frac{\begin{array}{c} 0.2753z^7 - 2.0020z^6 + 11.0993z^5 - 32.4331z^4 + 117.5229z^3 - 129.7845z^2 - 12.2294z^1 \\ 63.7094z^0 - 22.9293z^{-1} + 16.1668z^{-2} - 5.8734z^{-3} - 4.0484z^{-4} + 1.9430z^{-5} - 0.7235z^{-6} \\ 0.2003z^{-7} - 0.0369z^{-8} + 0.0034z^{-9} \end{array}}{1 - 0.1401z^{-1}}.$$

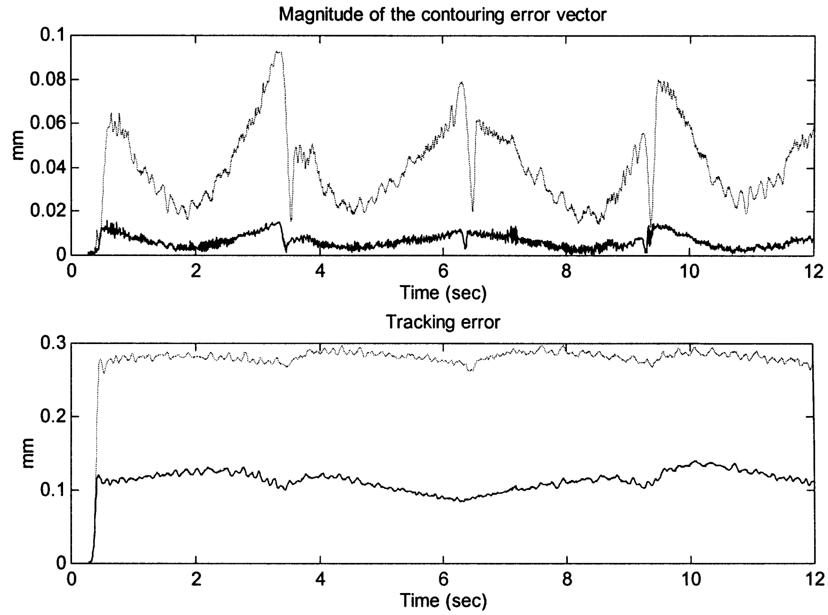

Fig. 9. Experimental results of the three-axis motion system for different structures: Case 1): P controller (dashed). Case 4): integrated controller (solid).

TABLE I
EXPERIMENTAL RESULTS OF THE THREE-AXIS MOTION CONTROL SYSTEM

Performance index / Control system	Contouring error (mm)				Tracking error (mm)			
	Max	Mean	IAE	RMS	Max	Mean	IAE	RMS
Case(1) P Feedback	0.093	0.040	79.344	0.044	0.298	0.273	544.96	0.277
Case(2) P+ Feedforward, w/o CCC	0.090	0.040	78.632	0.043	0.132	0.115	230.28	0.117
Case(3) P + CCC, w/o Feedforward	0.016	0.006	12.551	0.007	0.304	0.269	538.84	0.274
Case(4) Integrated, CCC + Feedforward	0.016	0.006	12.669	0.007	0.140	0.110	220.41	0.113

The QFT algorithm [12] was applied to obtain a robust CCC design

$$K_c\left(z^{-1}\right) = \frac{0.05 - 0.09z^{-1} + 0.040\,375z^{-2}}{1 - 1.03z^{-1} + 0.0302z^{-2} - 0.0002z^{-3}}$$

and the obtained frequency responses of KK_c, shown on the inverse Nichol's chart in Fig. 7, easily meet the conservative design specifications as C varies within $[-1, 1]$.

C. Experimental Results

The present position commands performed an inclined circular contour with a 18.75 mm radius at a speed of 600 mm/min for the three-axis machining center, as shown in Fig. 8 [17]. Experimental results for four control structures are shown in Fig. 9 and Table I. Compared with the well-tuned P control structure provided by the manufacturer, results indicate that contouring accuracy is greatly improved but the tracking accuracy is about the same by applying the CCC only, as in Case (3). Moreover, results also indicates that tracking error in Case (2) is significantly reduced as the feedforward controller is applied; however, the contouring error is about the same if the CCC is not applied. Similar to results obtained for biaxial systems [15], the present integrated control as in Case (4), which is formulated for general multi-axis systems, including all feedback loops, feedforward loops, and CCC, provides both the best tracking and contouring accuracy simultaneously as shown in Fig. 10.

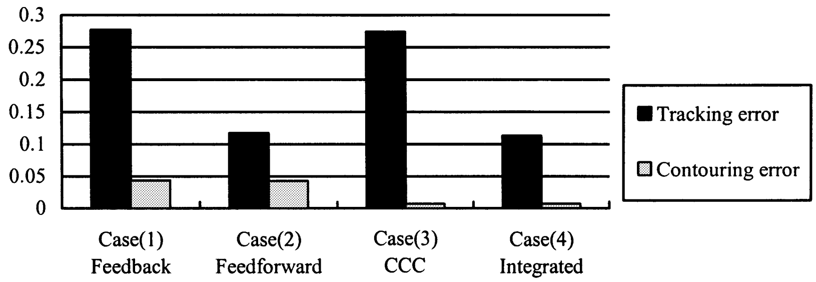

Fig. 10. Tracking and contouring errors in rms.

VI. Conclusion

In this paper, we provide analysis and systematic design procedures for the integrated controller. Since the tracking error is reduced by applying the feedforward and feedback controllers, the contouring error accordingly decreases. Furthermore, the formulation of CETF for integrated control systems leads to an efficient design as in a simple SISO control system. The robust design of the integrated system provides sufficient stability margins to overcome the parameter-varying control design problem in real applications. Note that although the proposed multi-axis integrated control design is based on the decoupled motion axes, the proposed approach is also suitable for MIMO motion systems with prior decoupling control. Theoretical analysis and experimental results show that the proposed formulation and control design significantly improve motion accuracy for multi-axis motion systems.

References

[1] A. Poo, J. G. Bollinger, and W. Younkin, "Dynamic error in type contouring systems," *IEEE Trans. Ind. Applicat.*, vol. IA-8, no. 4, pp. 477–484, 1972.

[2] M. Tomizuka, "Zero phase error tracking algorithm for digital control," *ASME Trans. J. Dyn. Syst., Meas. Contr.*, vol. 109, pp. 65–68, 1987.

[3] T. C. Tsao and M. Tomizuka, "Robust adaptive and repetitive digital tracking control and application to a hydraulic servo for noncircular machining," *ASME Trans. J. Dyn. Syst., Meas. Contr.*, vol. 116, pp. 24–32, 1994.

[4] J. Z. Xia and C. H. Menq, "Precision tracking control of nonminimum phase systems with zero phase error," *Int. J. Contr.*, vol. 61, no. 4, pp. 791–807, 1995.

[5] S. S. Yeh and P. L. Hsu, "An optimal and adaptive design of the feedforward motion controller," *IEEE/ASME Trans. Mechatron.*, vol. 4, no. 4, pp. 428–439, 1999.

[6] Y. Koren, "Cross-Coupled biaxial computer for manufacturing systems," *ASME Trans. J. Dyn. Syst., Meas. Contr.*, vol. 102, no. 4, pp. 265–272, 1980.

[7] H. Y. Chuang and C. H. Liu, "Cross-Coupled adaptive feedrate control for multiaxis machine tools," *ASME Trans. J. Dyn. Syst., Meas. Contr.*, vol. 113, no. 3, pp. 451–457, 1991.

[8] P. K. Kulkarni and K. Srinivasan, "Optimal contouring control of multi-axis drive servomechanisms," *ASME Trans. J. Dyn. Syst., Meas., Contr.*, vol. 111, no. 2, pp. 140–148, 1989.

[9] ——, "Cross-Coupled control of biaxial feed drive servomechanisms," *ASME Trans. J. Dyn. Syst., Meas., Contr.*, vol. 112, no. 2, pp. 225–232, 1990.

[10] Y. Koren and C. C. Lo, "Variable gain cross coupling controller for contouring," in *Proc. CIRP Manufact. Syst.*, vol. 40, 1991, pp. 371–374.

[11] ——, "Advanced controllers for feed drives," in *Proc. CIRP Manufact. Syst.*, vol. 41, 1992, pp. 689–698.

[12] S. S. Yeh and P. L. Hsu, "Theory and applications of the robust cross-coupled control design," *ASME Trans. J. Dyn. Syst., Meas., Contr.*, vol. 121, no. 3, pp. 524–530, 1999.

[13] C. C. Lo, "Three-Axis contouring control based on a trajectory coordinate basis," *JSME Int. J. Ser. C Mech. Syst. Machine Elements Manufact.*, vol. 41, no. 2, pp. 242–247, 1998.

[14] G. T. C. Chiu and M. Tomizuka, "Contouring control of machine tool feed drive systems: A task coordinate frame approach," *IEEE Trans. Contr. Syst. Technol.*, vol. 9, pp. 130–139, Jan. 2001.

[15] S. S. Yeh and P. L. Hsu, "Analysis and design of the integrated controller for precise motion systems," *IEEE Trans. Contr. Syst. Technol.*, vol. 7, pp. 706–717, Nov. 1999.

[16] Y. Y. Chang and P. L. Hsu, "The design of precise motion systems by applying both the advanced controllers and the interpolators," in *Proc. 6th Int. Workshop Advanced Motion Contr.*, Nagoya, Japan, Mar. 2000, pp. 240–245.

[17] S. S. Yeh and P. L. Hsu, "Estimation of the contouring error vector for the cross-coupled control design," *IEEE/ASME Trans. Mechatron.*, vol. 7, no. 1, pp. 44–51, 2002.

[18] S. S. Yeh, "Design Of Integrated Controllers and Parametric Interpolators for Multi-Axis Motion Systems," Ph.D. dissertation, Inst. Electr. Contr. Eng., NCTU, 2000.

[19] K. S. Tsaklis and P. A. Ioannou, *Linear Time-Varying Systems*. Englewood Cliffs, NJ: Prentice-Hall, 1993.

[20] C. A. Desoer, "Slowly varying system," *IEEE Trans. Automat. Contr.*, vol. AC-14, pp. 780–781, June 1969.

[21] T. Söderström and P. Stoica, *System Identification*. Englewood Cliffs, NJ: Prentice-Hall, 1989.